Computers and Mathematics with Applications 75 (2018) 2002–2016

Contents lists available at ScienceDirect

Computers and Mathematics with Applications

journal homepage: www.elsevier.com/locate/camwa

Nonconforming immersed finite element spaces for elliptic interface problems[☆]

Ruchi Guo [a,*], Tao Lin [a], Xu Zhang [b]

[a] Department of Mathematics, Virginia Tech, Blacksburg, VA 24061, United States
[b] Department of Mathematics and Statistics, Mississippi State University, Mississippi State, MS 39762, United States

A R T I C L E   I N F O

Article history:
Available online 7 December 2017

Keywords:
Interface problems
Immersed finite element
Nonconforming
Interpolation error estimates

A B S T R A C T

In this paper, we use a unified framework introduced in Chen and Zou (1998) to study two nonconforming immersed finite element (IFE) spaces with integral-value degrees of freedom. The shape functions on interface elements are piecewise polynomials defined on sub-elements separated either by the actual interface or its line approximation. In this unified framework, we use the invertibility of the well known Sherman–Morison systems to prove the existence and uniqueness of IFE shape functions on each interface element in either a rectangular or triangular mesh. Furthermore, we develop a multi-edge expansion for piecewise functions and a group of identities for nonconforming IFE functions which enable us to show the optimal approximation capability of these IFE spaces.

1. Introduction

Consider the classical second-order elliptic interface problem:

$$-\nabla\cdot(\beta\nabla u)=f, \quad \text{in } \Omega^-\cup\Omega^+, \tag{1.1}$$

$$u=g, \quad \text{on } \partial\Omega, \tag{1.2}$$

where the domain $\Omega \subseteq \mathbb{R}^2$ is assumed to be separated by an interface curve Γ into two subdomains Ω^+ and Ω^-. The diffusion coefficient $\beta(X)$ is a piecewise constant:

$$\beta(X)=\begin{cases}\beta^- & \text{if } X\in\Omega^-,\\ \beta^+ & \text{if } X\in\Omega^+,\end{cases}$$

and the exact solution u is required to satisfy the jump conditions:

$$[u]_\Gamma = 0, \tag{1.3}$$

$$\left[\beta\nabla u\cdot\mathbf{n}\right]_\Gamma = 0, \tag{1.4}$$

where $\mathbf{n}$ is the unit normal vector to the interface Γ. Here and from now on, for every piecewise function v defined as

$$v=\begin{cases}v^-(X) & \text{if } X\in\Omega^-,\\ v^+(X) & \text{if } X\in\Omega^+,\end{cases}$$

we adopt the notation $[v]|_\Gamma = v^+|_\Gamma - v^-|_\Gamma$.

☆ This work is partially supported by NSF grant DMS-1720425.

* Corresponding author.
E-mail addresses: ruchi91@vt.edu (R. Guo), tlin@math.vt.edu (T. Lin), xuzhang@math.msstate.edu (X. Zhang).

https://doi.org/10.1016/j.camwa.2017.10.040
0898-1221/

The IFE method was introduced in [1] for solving an 1D elliptic interface problem with meshes independent of the interface. Extensions to 2D elliptic interface problems include IFE functions defined by conforming P_1 polynomials [2–6], conforming Q_1 polynomials [7–10], nonconforming P_1 (Crouzeix–Raviart) polynomials [11], and nonconforming rotated-Q_1 (Rannacher–Turek) polynomials [12–14]. IFE shape functions in these articles are H^1 functions defined with a line approximating the original interface curve in each interface element. Recently, the authors in [15,16] developed IFE spaces according to the original interface curve where the local degrees of freedom are of Lagrange type. The goal of this article is to develop and analyze IFE spaces constructed with the actual interface curve and the degrees of freedom as the integral values on element edges.

There are two motivations for us to consider IFE functions with integral-value degrees of freedom and with the actual interface curve instead of its line approximation. First, as observed in [13,14], IFE functions of this non-Lagrange type usually have less severe discontinuity across interface edges because their continuity across an element edge is weakly enforced over the entire edge in an average sense. Compared to Lagrange type IFE spaces, the IFE spaces with integral-value degrees of freedom, such as the one considered in [13], usually do not require additional penalty terms in order to obtain accurate approximation in both the actual computation and the error analysis. This important feature is corroborated by numerical examples in this article and [14].

The second motivation is our desire to develop higher degree IFE spaces for which using a line to approximate the interface curve is not sufficient anymore because of the $O(h^2)$ accuracy limitation for the line to approximate a curve. Recently, we have constructed high order immersed finite element spaces based on curve partition using the least squares method [17]. Even though the analysis for IFE functions in this article is still for lower degree nonconforming P_1 or rotated-Q_1 polynomials, we hope our investigation can serve as a precursor to the development of higher degree IFE spaces. In addition, we will demonstrate later that the framework presented here can also be applied to nonconforming IFE spaces based on the line partitioning [11,13,14].

Even though the new IFE spaces presented here seem to be natural because they are constructed locally on each interface element according to the actual interface curve of the problem to be solved, the related investigation faces a few hurdles. The first one is that the new IFE functions are discontinuous in each interface element except for trivial interface geometry because, in general, two distinct polynomials cannot perfectly match each other on a curve. In contrast, almost all IFE spaces in the literature are continuous in each element. This lack of continuity leads to a lower regularity of IFE functions in interface elements such that related error analysis demands new approaches different from those in the literature [5,8,14,18,19]. Another issue is that the interpolation error analysis technique based on the multi-point Taylor expansion in the literature is not applicable here because new IFE functions are constructed with integral-value degrees of freedom instead of the Lagrange type degrees of freedom.

The rest of this article is organized as follows. In Section 2, we introduce some basic notations, assumptions and known results to be used in this article. In Section 3, we extend the multi-point Taylor expansion established in [5,7,14,16] to a multi-edge expansion for piecewise C^2 functions such that the new expansion can handle integral-value degrees of freedom. Estimates for remainders in this new expansion are also derived in this section. In Section 4, we show that the integral-value degrees of freedom imposed on each edge and the approximated jump conditions together yield a Sherman–Morrison system for determining coefficients in an IFE shape function on interface elements. We show that the unisolvence and boundedness of IFE shape functions follow from the well-known invertibility of the Sherman–Morrison system. A group of fundamental identities such as partition of unity are also derived for new IFE shape functions. In Section 5, we establish the optimal approximation capability for IFE spaces with the integral-value degrees of freedom defined either according to the actual interface or to a line approximating the interface curve [11,14]. In Section 6, we present some numerical examples.

2. Preliminaries

Throughout this article, we adopt the notations used in [16], and we recall some of them for reader's convenience. We assume that $\Omega \subset \mathbb{R}^2$ is a bounded domain that is a union of finitely many rectangles, and that Ω is separated by an interface curve Γ into two subdomains Ω^+ and Ω^- such that $\overline{\Omega} = \overline{\Omega^+} \cup \overline{\Omega^-} \cup \Gamma$. For any measurable subset $\tilde{\Omega} \subseteq \Omega$, we consider the standard Sobolev spaces $W^{k,p}(\tilde{\Omega})$ and the associated norm $\|\cdot\|_{k,p,\tilde{\Omega}}$ and semi-norm $|v|_{k,p,\tilde{\Omega}}$. The corresponding Hilbert space is $H^k(\tilde{\Omega}) = W^{k,2}(\tilde{\Omega})$. When $\tilde{\Omega}^s = \tilde{\Omega} \cap \Omega^s \neq \emptyset$, $s = \pm$, we let

$$PW^{k,p}_{int}(\tilde{\Omega}) = \{u : u|_{\tilde{\Omega}^s} \in W^{k,p}(\tilde{\Omega}^s),\ \ s = \pm;\ \ [u] = 0 \text{ and } [\beta \nabla u \cdot \mathbf{n}_\Gamma] = 0 \text{ on } \Gamma \cap \tilde{\Omega}\},$$

$$PC^{k}_{int}(\tilde{\Omega}) = \{u : u|_{\tilde{\Omega}^s} \in C^{k}(\tilde{\Omega}^s),\ \ s = \pm;\ \ [u] = 0 \text{ and } [\beta \nabla u \cdot \mathbf{n}_\Gamma] = 0 \text{ on } \Gamma \cap \tilde{\Omega}\},$$

with the associated norms and semi-norms:

$$\|\cdot\|^p_{k,p,\tilde{\Omega}} = \|\cdot\|^p_{k,p,\tilde{\Omega}^+} + \|\cdot\|^p_{k,p,\tilde{\Omega}^-}, \qquad |\cdot|^p_{k,p,\tilde{\Omega}} = |\cdot|^p_{k,p,\tilde{\Omega}^+} + |\cdot|^p_{k,p,\tilde{\Omega}^-}.$$

Specifically, if $p = 2$, we have the corresponding Hilbert space $PH^2_{int}(\tilde{\Omega})$ with the norms $\|\cdot\|_{k,\tilde{\Omega}}$ and semi-norms $|\cdot|_{k,\tilde{\Omega}}$. When $p = \infty$, we define

$$\|\cdot\|_{k,\infty,\tilde{\Omega}} = \max(\|\cdot\|_{k,\infty,\tilde{\Omega}^+},\ \|\cdot\|_{k,\infty,\tilde{\Omega}^-}), \qquad |\cdot|_{k,\infty,\tilde{\Omega}} = \max(|\cdot|_{k,\infty,\tilde{\Omega}^+},\ |\cdot|_{k,\infty,\tilde{\Omega}^-}).$$

Let $\mathcal{T}_h$ be a Cartesian triangular or rectangular mesh of the domain Ω with the maximum length of edge h. An element $T \in \mathcal{T}_h$ is called an interface element provided the interior of T intersects with the interface Γ; otherwise, we name it a non-interface element. We let $\mathcal{T}^i_h$ and $\mathcal{T}^n_h$ be the set of interface elements and non-interface elements, respectively. Similarly, $\mathcal{E}^i_h$ and $\mathcal{E}^n_h$ are sets of interface edges and non-interface edges, respectively. Besides, we assume that $\mathcal{T}_h$ satisfies the following hypotheses [20], when the mesh size h is small enough:

- **(H1)** The interface Γ cannot intersect an edge of any element at more than two points unless the edge is part of Γ.
- **(H2)** The interface Γ can only intersect the boundary of an interface element at two points, and these intersection points must be on different edges of this element.
- **(H3)** The interface Γ is a piecewise C^2 function, and the mesh $\mathcal{T}_h$ is formed such that the subset of Γ in every interface element $T \in \mathcal{T}^i_h$ is C^2- continuous.
- **(H4)** The interface Γ is smooth enough so that $PC^2_{int}(T)$ is dense in $PH^2_{int}(T)$ for every interface element $T \in \mathcal{T}^i_h$.

In addition, in the following discussion, all the elements T and the corresponding subelements $T^{\pm} = T \cap \overline{\Omega^{\pm}}$ are considered as closed sets.

On an element $T \in \mathcal{T}_h$, we consider the local finite element space (T, Π_T, Σ_T) with

$$\Pi_T = \begin{cases} \text{Span}\{1, x, y\}, & \text{for Crouzeix–Raviart (C–R) finite element functions,} \\ \text{Span}\{1, x, y, x^2 - y^2\}, & \text{for rotated-}Q_1 \text{ finite element functions,} \end{cases} \tag{2.1}$$

$$\Sigma_T = \left\{ \frac{1}{|b_i|} \int_{b_i} \psi_T(X) ds : i \in \mathcal{I},\ \forall \psi_T \in \Pi_T \right\}, \tag{2.2}$$

where $\mathcal{I} = \{1, 2, \ldots, DOF(T)\}$ is the index set with $DOF(T) = 3, 4$ depending on whether T is triangular or rectangular and $b_i, i \in \mathcal{I}$ are edges of the element T. In addition, let M_i be the midpoint of the edge b_i, $i \in \mathcal{I}$. Recall from [21] that (T, Π_T, Σ_T) has a set of shape functions $\psi_{i,T}$, $i \in \mathcal{I}$ such that

$$\frac{1}{|b_j|} \int_{|b_j|} \psi_{i,T}(X) ds = \delta_{ij}, \quad \left\|\psi_{i,T}\right\|_{\infty,T} \le C, \quad \left\|\nabla\psi_{i,T}\right\|_{\infty,T} \le Ch^{-1}, \quad i, j \in \mathcal{I}, \tag{2.3}$$

where δ_{ij} is the *Kronecker* delta function.

Furthermore, we let $\rho = \beta^-/\beta^+$, and on every $T \in \mathcal{T}^i_h$ we use D, E to denote the intersection points of Γ and ∂T, and let l be the line connecting D and E. Let $\bar{\mathbf{n}} = (\bar{n}_x, \bar{n}_y)^t$ and $\mathbf{n}(\widetilde{X}) = (\tilde{n}_x(\widetilde{X}), \tilde{n}_y(\widetilde{X}))^t$ be the normal vector to l and to Γ at $\widetilde{X} \in \Gamma$, respectively. In the following discussion, s is the index that is either $-$ or $+$, and s' takes the opposite sign whenever a formula have them both. Let F be an arbitrary point either on the line l or the interface curve $\Gamma \cap T$. We associate the point F with a vector $\mathbf{v}(F) = (v_x(F), v_y(F))^t$ such that the following two cases will be considered:

1. If $F \in \Gamma \cap T$ but $F \ne D, E$, then $\mathbf{v}(F) = \mathbf{n}(F)$ and T is partitioned by Γ into two subelements $T^s_{curve} = T^s$, $s = \pm$.
2. If $F \in l$, then let $\mathbf{v}(F) = \bar{\mathbf{n}}$ and T is partitioned by l into two subelements T^s_{line}, $s = \pm$.

Lemma 3.1 and Remark 3.1 in [16] provide a critical ingredient in our analysis: on a mesh fine enough, there exists a constant C such that

$$\mathbf{v}(F) \cdot \bar{\mathbf{n}} \geqslant 1 - Ch^2. \tag{2.4}$$

As in [16], we will employ the following matrices:

$$M^s(\widetilde{X}) = \begin{pmatrix} \tilde{n}^2_y(\widetilde{X}) + \beta^s/\beta^{s'}\tilde{n}^2_x(\widetilde{X}) & (\beta^s/\beta^{s'} - 1)\tilde{n}_x(\widetilde{X})\tilde{n}_y(\widetilde{X}) \\ (\beta^s/\beta^{s'} - 1)\tilde{n}_x(\widetilde{X})\tilde{n}_y(\widetilde{X}) & \tilde{n}^2_x(\widetilde{X}) + \beta^s/\beta^{s'}\tilde{n}^2_y(\widetilde{X}) \end{pmatrix}, \tag{2.5}$$

$$\overline{M}^s(F) = \frac{1}{\bar{\mathbf{n}} \cdot \mathbf{n}(F)} \begin{pmatrix} \bar{n}_y n_y(F) + \beta^s/\beta^{s'}\bar{n}_x v_x(F) & -\bar{n}_x v_y(F) + \beta^s/\beta^{s'}\bar{n}_x v_y(F) \\ -\bar{n}_y n_x(F) + \beta^s/\beta^{s'}\bar{n}_y v_x(F) & \bar{n}_x v_x(F) + \beta^s/\beta^{s'}\bar{n}_y v_y(F) \end{pmatrix}, \tag{2.6}$$

where $s = \pm$ and $\overline{M}^s(F)$ is well defined since (2.4) implies that $\bar{\mathbf{n}} \cdot \mathbf{n}(F) > 0$ when h is small enough.

3. Multi-edge Taylor expansion on interface elements

In this section, we derive a multi-edge expansion for a function u on an interface element to handle integral-value degrees of freedom. We will show that the integral value $\frac{1}{|b_i|}\int_{b_i} u(X)ds$, $i \in \mathcal{I}$ can be expressed in terms of u and its derivatives for various configurations of the interface and edges. Estimates for the remainders of this expansion will be given.

We partition the index set $\mathcal{I}$ into three subsets $\mathcal{I}^- = \{i : b_i \subseteq T^-\}, \mathcal{I}^+ = \{i : b_i \subseteq T^+\}$ and $\mathcal{I}^{int} = \{i : b_i \cap T^s \neq \emptyset, s = \pm\}$. Given an edge b_i, for every point $P \in b_i$ and $X \in T$, we note that $Y_i(t, P, X) = tP + (1-t)X, t \in [0, 1]$ is a point on the line segment connecting P and X. We note that for some points X and P, the line $\overline{PX}$ may intersect the curve $\Gamma \cap T$ at multiple points. Define

$$T_{int} = \{X \in T : \text{there exists a point } Y \in T \cap \Gamma, \text{ such that } \overline{XY} \text{ is a tangent line to } \Gamma \text{ at } Y\}$$

which is actually formed by the line segments inside T each of which is tangent to $T \cap \Gamma$ at an end point $Y \in \Gamma \cap T$. Lemma 3.1 in [16] shows that $|T_{int}| \leqslant Ch^3$ when the mesh is fine enough.

First we derive the multi-edge expansion for a point $X \in T_{non} = T \setminus T_{int}$. For convenience, we define $T^s_{non} = T_{non} \cap T^s$. We note that for any $P \in \partial T$, the line segment $\overline{PX}$ intersects with $\Gamma \cap T$ either at no point or at just one point. In the second case, X and P sit on different sides of $\Gamma \cap T$ and we denote the intersection point by $\widetilde{Y}_i = Y_i(\tilde{t}, P, X)$ for a $\tilde{t}_i = \tilde{t}_i(P, X) \in [0, 1]$. Consider a piecewise defined function $R_i : b_i \times T_{non} \to \mathbb{R}$, given by

$$R_i(P,X) = \begin{cases} \displaystyle\int_0^1 (1-t)\frac{d^2}{dt^2}u^s(Y_i(t,P,X))dt, & \text{if } P \in T^s \cap b_i,\ X \in T^s_{non}, \\ R_{i1}(P,X) + R_{i2}(P,X) + R_{i3}(P,X), & \text{if } P \in T^{s'} \cap b_i,\ X \in T^s_{non}, \end{cases} \tag{3.1}$$

where

$$\begin{cases} R_{i1}(P,X) = \displaystyle\int_0^{\tilde{t}_i} (1-t)\frac{d^2u^s}{dt^2}(Y_i(t,P,X))dt, \\ R_{i2}(P,X) = \displaystyle\int_{\tilde{t}_i}^1 (1-t)\frac{d^2u^{s'}}{dt^2}(Y_i(t,P,X))dt, \\ R_{i3}(P,X) = (1-\tilde{t}_i)\displaystyle\int_0^{\tilde{t}_i} \frac{d}{dt}\left((M^s(\widetilde{Y}_i) - I)\nabla u^s(Y_i(t,X)) \cdot (P-X)\right)dt. \end{cases} \tag{3.2}$$

For $u \in PC^2_{int}(T)$, recall the following multi-point Taylor expansion formulation and the estimates of (3.1) and (3.2) from [16]:

$$u^s(P) = u^s(X) + \nabla u^s(X)\cdot(P-X) + R_i(P,X), \text{ if } P \in T^s \cap b_i,\ X \in T^s_{non}, \tag{3.3}$$

$$\begin{aligned} u^{s'}(P) =& u^s(X) + \nabla u^s(X)\cdot(P-X) + \left(\left(M^s(\widetilde{Y}_i) - I\right)\nabla u^s(X)\right)\cdot(P-\widetilde{Y}_i) \\ &+ R_i(P,X), \text{ if } P \in T^{s'} \cap b_i,\ X \in T^s_{non}, \end{aligned} \tag{3.4}$$

and for any fixed $P \in b_i$,

$$\|R_i(P,\cdot)\|_{0,T^s_{non}} \leqslant Ch^2|u|_{2,T},\ s = \pm,\ \forall i \in \mathcal{I}. \tag{3.5}$$

Integrating (3.3) and (3.4) on each edge b_i with respect to P, we obtain the following multi-edge expansion for $u^s(X)$ with $X \in T^s_{non}$:

$$\frac{1}{|b_i|}\int_{b_i} u^s(P)ds(P) = u^s(X) + \nabla u^s(X)\cdot(M_i - X) + \mathcal{R}_i(X),\ i \in \mathcal{I}^s, \tag{3.6}$$

$$\begin{aligned} \frac{1}{|b_i|}\int_{b_i} u^{s'}(P)ds(P) =& u^s(X) + \nabla u^s(X)\cdot(M_i - X) + \mathcal{R}_i(X) \\ &+ \frac{1}{|b_i|}\int_{b_i}\left(\left(M^s(\widetilde{Y}_i) - I\right)\nabla u^s(X)\right)\cdot(P-\widetilde{Y}_i)ds(P),\ i \in \mathcal{I}^{s'}, \end{aligned} \tag{3.7}$$

$$\begin{aligned} \frac{1}{|b_i|}\int_{b_i} u(P)ds(P) =& u^s(X) + \nabla u^s(X)\cdot(M_i - X) + \mathcal{R}_i(X) \\ &+ \frac{1}{|b_i|}\int_{b_i\cap T^{s'}}\left(\left(M^s(\widetilde{Y}_i) - I\right)\nabla u^s(X)\right)\cdot(P-\widetilde{Y}_i)ds(P),\ i \in \mathcal{I}^{int}, \end{aligned} \tag{3.8}$$

where

$$\mathcal{R}_i(X) = \frac{1}{|b_i|}\int_{b_i} R_i(P,X)ds(P). \tag{3.9}$$

Now we estimate these reminders $\mathcal{R}_i$.

Lemma 3.1. *Assume $u \in PC^2_{int}(T)$, then there exists a constant C independent of the interface location, such that*

$$\|\mathcal{R}_i\|_{0,T^s_{non}} \leqslant Ch^2|u|_{2,T},\ s=\pm,\ \forall i \in \mathcal{I}. \tag{3.10}$$

Proof. By the estimate (3.5) and Minkowski inequality, we have

$$\begin{aligned}\|\mathcal{R}_i\|_{0,T^s_{non}} =&\left(\int_{T^s_{non}}\left(\frac{1}{|b_i|}\int_{b_i} R_i(P,X)ds(P)\right)^2 dX\right)^{\frac{1}{2}}\\ \leqslant&\frac{1}{|b_i|}\int_{b_i}\left(\int_{T^s_{non}}(R_i(P,X))^2dX\right)^{\frac{1}{2}}ds(P)\\ \leqslant&\frac{Ch^2}{|b_i|}\int_{b_i}|u|_{2,T}\ ds(P)\leqslant Ch^2|u|_{2,T}.\qquad\square\end{aligned}$$

We now consider the multi-edge expansion for $X \in T_{int}$. We start from the following first order multi-point Taylor expansion for every $u \in PC^2_{int}(T)$:

$$u^s(P) = u^s(X) + R_i(P,X),\qquad X\in T_{int},\ P\in b_i,\ i\in\mathcal{I}, \tag{3.11}$$

where $R_i : b_i \times T_{int} \to \mathbb{R}$ is a function defined by

$$R_i(P,X) = \int_0^1 \frac{du}{dt}(Y_i(t,P,X))dt = \int_0^1 \nabla u(Y_i(t,P,X))\cdot(P-X)dt. \tag{3.12}$$

Integrating (3.12) on each edge b_i with respect to P, we obtain the following multi-edge expansion:

$$\frac{1}{|b_i|}\int_{b_i} u(P)ds(P) = u(X) + \mathcal{R}_i(X),\ \ i\in\mathcal{I},\quad \text{where}\ \ \mathcal{R}_i(X) = \frac{1}{|b_i|}\int_{b_i} R_i(P,X)ds(P). \tag{3.13}$$

According to Sobolev embedding theorems, since $u \in H^2(T^s)$, we have $u \in W^{1,6}(T^s)$, $s=\pm$. Hence we can estimate the reminders in (3.13) in terms of the norms $\|\cdot\|_{1,6,T}$.

Lemma 3.2. *Assume $u \in PH^2_{int}(T)$, then there exists a constant C independent of the interface location such that for the fixed t*

$$\|R_i(P,\cdot)\|_{0,T_{int}} \leqslant Ch^2\|u\|_{1,6,T}. \tag{3.14}$$

Proof. We consider the linear mapping $\xi : X \to \hat{X} = tP + (1-t)X$ for $t \in [0,1]$ and $P \in b_i$ which maps T_{int} to

$$\hat{T}_{int}(t) = \{tP + (1-t)X : X \in T_{int}\}.$$

Since ξ is a linear mapping, $|\hat{T}_{int}(t)| = (1-t)^2|T_{int}| \leqslant C(1-t)^2h^3$. Now by Hölder's inequality and following the similar idea employed in [22], we have

$$\begin{aligned}\left(\int_{T_{int}}(\nabla u(Y_i)\cdot(P-X))^2dX\right)^{1/2} &\leqslant Ch\left(\int_{T_{int}}|\nabla u(Y_i(t,P,X))|^2dX\right)^{1/2}\\ &= C(1-t)^{-1}h\left(\int_{\hat{T}_{int}}\left|\nabla u(\hat{X})\right|^2 d\hat{X}\right)^{1/2}\\ &\leqslant C(1-t)^{-1}h\left(\int_{\hat{T}_{int}}1^{3/2}d\hat{X}\right)^{1/3}\left(\int_{\hat{T}_{int}}|\nabla u(\hat{X})|^6 d\hat{X}\right)^{1/6}\\ &\leqslant C(1-t)^{-1/3}h^2\|u\|_{1,6,T}.\end{aligned}$$

Then by Minkowski's inequality and the estimate above, we have

$$\begin{aligned}\|R_i(P,\cdot)\|_{0,T_{int}} =&\left(\int_{T_{int}}\left(\int_0^1\nabla u(Y_i)\cdot(P-X)dt\right)^2dX\right)^{1/2}\\ \leqslant&\int_0^1\left(\int_{T_{int}}(\nabla u(Y_i)\cdot(P-X))^2dX\right)^{1/2}dt\\ \leqslant& Ch^2\|u\|_{1,6,T}\int_0^1(1-t)^{-1/3}dt = \frac{3C}{2}h^2\|u\|_{1,6,T}\end{aligned}$$

which completes the proof. $\square$

Finally, we give estimates for the remainder in the multi-edge expansion (3.13) in the following lemma.

Lemma 3.3. *Assume $u \in PH^2_{int}(T)$, then there exists a constant C independent of the interface location such that*

$$\|\mathcal{R}_i\|_{0,T_{int}} \leqslant Ch^2 \|u\|_{1,6,T}, \ i \in \mathcal{I}. \tag{3.15}$$

Proof. The result follows from Lemma 3.2 and arguments similar to those used in the proof for Lemma 3.1. □

4. IFE spaces and their properties

In this section, we use the finite element space (T, Π_T, Σ_T) for $T \in \mathcal{T}_h$ described in (2.1) and (2.2) to develop the nonconforming P_1 and rotated Q_1 IFE spaces with integral-value degrees of freedom. First we prove the unisolvence of the IFE shape functions on interface elements by the invertibility of the Sherman–Morison system. Then we present a few properties of IFE spaces which play important roles in the analysis of approximation capabilities. We note the framework presented here provides a unified approach for both nonconforming P_1 and rotated Q_1 IFE spaces developed in the literature [11,13,14] and the new ones defined with the actual interface curve.

4.1. Construction of IFE spaces

First, on every element $T \in \mathcal{T}_h$, we have the standard local finite element space

$$S_h^{non}(T) = \text{Span}\{\psi_{i,T} : \ i \in \mathcal{I}\}, \tag{4.1}$$

where $\psi_{i,T}, i \in \mathcal{I}$ are the shape functions satisfying (2.3). Naturally (4.1) can be used as the local IFE space on each non-interface element $T \in \mathcal{T}_h^n$. So we focus on constructing the local IFE space on every interface element.

The main task is to construct IFE shape functions on an arbitrary interface element $T \in \mathcal{T}_h^i$. We consider the IFE functions in the following form of piecewise polynomials

$$\phi_T(X) = \begin{cases} \phi_T^-(X) \in \Pi_T & \text{if } \ X \in T_p^-, \\ \phi_T^+(X) \in \Pi_T & \text{if } \ X \in T_p^+, \end{cases} \tag{4.2}$$

where $p = curve$ or $line$, as described in Section 2, such that the jump conditions (1.3) and (1.4) are satisfied in the following approximate sense:

$$\begin{cases} \phi_T^-|_l = \phi_T^+|_l, & \text{if } T \text{ is a triangular element}, \\ \phi_T^-|_l = \phi_T^+|_l, \ \ \partial_{xx}(\phi_T^-) = \partial_{xx}(\phi_T^+), & \text{if } T \text{ is a rectangular element}, \end{cases} \tag{4.3}$$

$$\beta^-\nabla\phi_T^-(F)\cdot\mathbf{v}(F) = \beta^+\nabla\phi_T^+(F)\cdot\mathbf{v}(F), \tag{4.4}$$

where F is an arbitrary point as described in Section 2 and l is the segment connecting the intersection points of the interface with edges of T. Let $\overline{\mathcal{I}^s} = \mathcal{I}^s \cup \mathcal{I}^{int}$, $s = \pm$. Without loss of generality, we assume that $\left|\overline{\mathcal{I}^-}\right| \leq \left|\overline{\mathcal{I}^+}\right|$. For an IFE function ϕ_T under the integral degrees of freedom constraints

$$\frac{1}{|b_i|}\int_{b_i} \phi_T(X)ds = v_i, \quad i \in \mathcal{I}, \tag{4.5}$$

the condition (4.3) implies that ϕ_T can be written in the following form

$$\phi_T(X) = \begin{cases} \phi_T^-(X) = \phi_T^+(X) + c_0 L(X) & \text{if } \ X \in T_p^-, \\ \phi_T^+(X) = \sum\limits_{i\in\overline{\mathcal{I}^-}} c_i\psi_{i,T}(X) + \sum\limits_{i\in\mathcal{I}^+} v_i\psi_{i,T}(X) & \text{if } \ X \in T_p^+, \end{cases} \tag{4.6}$$

where $L(X) = \bar{\mathbf{n}}\cdot(X - D)$ and $\nabla L(X) = \bar{\mathbf{n}}$. Then, applying the condition (4.4) to (4.6) leads to

$$c_0 = k\left(\sum_{i\in\overline{\mathcal{I}^-}} c_i\nabla\psi_{i,T}(F)\cdot\mathbf{v}(F) + \sum_{i\in\mathcal{I}^+} v_i\nabla\psi_{i,T}(F)\cdot\mathbf{v}(F)\right), \tag{4.7}$$

where $k = \left(\frac{1}{\rho} - 1\right)\frac{1}{\bar{\mathbf{n}}\cdot\mathbf{v}(F)}$ is well defined for h small enough, since $\bar{\mathbf{n}}\cdot\mathbf{v}(F) \geqslant 1 - Ch^2 > 0$ by Lemma 3.1 in [16]. Moreover we have

$$|k| \leq \left|\left(\frac{1}{\rho} - 1\right)\right| \frac{1}{1 - Ch^2}. \tag{4.8}$$

Substituting (4.7) into (4.6), setting (4.5) for $j \in \overline{\mathcal{I}^-}$ and using the first property in (2.3) for $i, j \in \overline{\mathcal{I}^-}$, we obtain

$$\begin{aligned} v_j = \frac{1}{h}\int_{b_j} \phi_T(X)ds &= \frac{1}{h}\int_{b_j\cap T^-} \left(\phi_T^+(X) + c_0 L(X)\right) ds + \frac{1}{h}\int_{b_j\cap T^+} \phi_T^+(X)ds \\ &= \frac{1}{h}\int_{b_j} \phi_T^+(X)ds + \frac{c_0}{h}\int_{b_j\cap T^-} L(X)ds \\ &= \sum_{i\in\overline{\mathcal{I}^-}} \left(\delta_{ij} + \frac{k}{h}\nabla\psi_{i,T}(F)\cdot\mathbf{v}(F)\int_{b_j\cap T^-} L(X)ds\right) c_i \\ &\quad + \frac{k}{h}\int_{b_j\cap T^-} L(X)ds \sum_{i\in\mathcal{I}^+} \left(\nabla\psi_{i,T}(F)\cdot\mathbf{v}(F)\right) v_i, \quad j \in \overline{\mathcal{I}^-} \end{aligned}$$

which can be written as a Sherman–Morrison system:

$$(I + k\,\boldsymbol{\delta}\boldsymbol{\gamma}^T)\mathbf{c} = \mathbf{b}, \tag{4.9}$$

for the unknown coefficients $\mathbf{c} = (c_i)_{i\in\overline{\mathcal{I}^-}}$, where

$$\boldsymbol{\gamma} = \left(\nabla\psi_{i,T}(F)\cdot\mathbf{v}(F)\right)_{i\in\overline{\mathcal{I}^-}}, \quad \boldsymbol{\delta} = \frac{1}{h}\left(\int_{b_i\cap T^-} L(X)ds\right)_{i\in\overline{\mathcal{I}^-}}, \tag{4.10}$$

$$\mathbf{b} = \left(v_i - \frac{k}{h}\int_{b_i\cap T^-} L(X)ds \sum_{j\in\mathcal{I}^+} \nabla\psi_{j,T}(F)\cdot\mathbf{v}(F)v_j\right)_{i\in\overline{\mathcal{I}^-}} \tag{4.11}$$

are all column vectors.

Now we present two lemmas that are fundamental for the unisolvence of the IFE shape functions in the proposed form.

Lemma 4.1. *For an interface element with arbitrary interface location and an arbitrary point $F \in l$, we have $\boldsymbol{\gamma}^T\boldsymbol{\delta} \in [0, 1]$.*

Proof. Because of the similarity, we only give the proof for the rectangular mesh. Without loss of generality, we consider the typical rectangle: $A_1 = (0, 0)$, $A_2 = (h, 0)$, $A_3 = (h, h)$, $A_4 = (0, h)$ with $b_1 = \overline{A_1A_2}$, $b_2 = \overline{A_2A_3}$, $b_3 = \overline{A_3A_4}$, $b_4 = \overline{A_4A_1}$. Taking into account of rotation, there are two possible interface elements that Γ cuts b_1 and b_4 or cuts b_1 and b_3. For simplicity, we only show the first case. And similar arguments apply to the second case. Let $D = (dh, 0)$ and $E = (0, eh)$, for some $d, e \in [0, 1]$ and $F = (td, (h - t)e)$, for some $t \in [0, h]$. Thus, $\bar{\mathbf{n}} = (e, d)/\sqrt{d^2 + e^2}$. By direct calculation, we have

$$\boldsymbol{\gamma}^T\boldsymbol{\delta} = \frac{de}{4(d^2+e^2)}\left(5(d^2+e^2) + 6(2t/h - 1)(d^2e - de^2) - 6de\right),$$

which shows that $\boldsymbol{\gamma}^T\boldsymbol{\delta}$ is linear in terms of t. Furthermore, by a direct verification, we have

$$\begin{aligned} \boldsymbol{\gamma}^T\boldsymbol{\delta} &= \frac{de}{4(d^2+e^2)}\left(5(d^2+e^2) - 6(d^2e - de^2) - 6de\right) \in [0, 1], \qquad \text{if } t = 0, \\ \boldsymbol{\gamma}^T\boldsymbol{\delta} &= \frac{de}{4(d^2+e^2)}\left(5(d^2+e^2) + 6(d^2e - de^2) - 6de\right) \in [0, 1], \qquad \text{if } t = h, \end{aligned}$$

and these guarantee $\boldsymbol{\gamma}^T\boldsymbol{\delta} \in [0, 1]$. □

Lemma 4.2. *For sufficiently small h, there exists a constant C depending only on ρ such that*

$$1 + k\,\boldsymbol{\gamma}^T\boldsymbol{\delta} \geq \min\left(1, \frac{1}{\rho}\right) - Ch. \tag{4.13}$$

Proof. We first consider the case $F \in l$ so that $\mathbf{v}(F) = \bar{\mathbf{n}}$, and thus, $k = 1/\rho - 1$. By Lemma 4.1, we have $1 + k\,\boldsymbol{\gamma}^T\boldsymbol{\delta} \geq \min\left(1, \frac{1}{\rho}\right)$, which implies (4.13) naturally. For the case $F \in \Gamma \cap T$, we introduce an auxiliary vector $\bar{\boldsymbol{\gamma}} = \left(\nabla\psi_{i,T}(F_\perp)\cdot\bar{\mathbf{n}}\right)_{i\in\overline{\mathcal{I}^-}}$ where $F_\perp$ is the orthogonal projection of F onto l. Then from Lemma 4.1, we have $\bar{\boldsymbol{\gamma}}^T\boldsymbol{\delta} \in [0, 1]$. Therefore, the proof essentially follows from the same argument as Lemma 3.1 in [16]. □

Theorem 4.1 (*Unisolvence*). *Let $\mathcal{T}_h$ be a mesh with h small enough. Then, on every element $T \in \mathcal{T}_h^i$, given any vector $v = (v_1, v_2, v_3, v_4) \in \mathbb{R}^4$ for the rotated Q_1 case (or $v = (v_1, v_2, v_3) \in \mathbb{R}^3$ for the C-R case), there exists a unique IFE function ϕ_T in the form of (4.6) satisfying the approximated jump conditions (4.3)–(4.4). Furthermore, we have the following explicit formula* *for the coefficients in the IFE shape functions:*

$$\mathbf{c} = \mathbf{b} - k\frac{(\boldsymbol{\gamma}^T\mathbf{b})\boldsymbol{\delta}}{1 + k\boldsymbol{\gamma}^T\boldsymbol{\delta}}. \tag{4.14}$$

Proof. Lemma 4.2 implies $1 + k\boldsymbol{\gamma}^T\boldsymbol{\delta} \neq 0$ for h small enough. Hence, the existence and uniqueness for coefficients $c_i, i \in \overline{\mathcal{I}^-}$ and c_0 as well as formula (4.14) follow straightforwardly from the well known properties of the *Sherman–Morrison* formula and (4.7). □

On each interface element T, Theorem 4.1 guarantees the existence and uniqueness of the IFE shape functions $\phi_{i,T}, i \in \mathcal{I}$ such that

$$\frac{1}{|b_j|}\int_{b_j} \phi_{i,T}(X)ds = \delta_{ij}, \quad i, j \in \mathcal{I}, \tag{4.15}$$

where δ_{ij} is the Kronecker delta function, which can be used to define the local IFE space as

$$S_h^{int}(T) = \text{Span}\{\phi_{i,T} : i \in \mathcal{I}\}. \tag{4.16}$$

As usual, the local IFE space can be employed to form a suitable global IFE function space on Ω in a finite element scheme. For example, we can consider the following global IFE space:

$$\begin{aligned} S_h(\Omega) = \Big\{ v \in L^2(\Omega) : v|_T \in S_h^{non}(T) \text{ if } T \in \mathcal{T}_h^n,\ v|_T \in S_h^{int}(T) \text{ if } T \in \mathcal{T}_h^i; \\ \int_e v|_{T_1}(P)ds(P) = \int_e v|_{T_2}(P)ds(P)\ \forall e \in \mathcal{E}_h,\ \ \forall T_1, T_2 \in \mathcal{T}_h \text{ such that } e \in T_1 \cap T_2 \Big\}. \end{aligned} \tag{4.17}$$

Remark 4.1. We note that if $\beta^- = \beta^+$, then $k = 0$ and $\mathbf{c} = \mathbf{b} = (v_i)_{i\in\mathcal{I}^-}$ such that the IFE shape function defined by (4.6) becomes its standard rotated Q_1 or linear finite element shape function counterpart. In addition, when $|T^-|$ or $|T^+|$ degenerates to 0, the whole element is occupied by only one piece of polynomials. This means the IFE shape function defined by (4.6) also becomes the corresponding rotated Q_1 or linear polynomial. These features have been called the consistence of the IFE shape functions [7,14].

Remark 4.2. Using the line partition of interface elements, the IFE function space obtained in (4.17) is identical to the nonconforming P_1 IFE space on triangular meshes [11] or the nonconforming rotated Q_1 IFE space on rectangular meshes [14].

4.2. Properties of the IFE shape functions

In this subsection, we present some fundamental properties for the IFE shape functions ϕ_T. The first two results are similar to those in Theorem 5.2 and Lemma 5.3 in [16] and the proofs of these results are essentially the same.

Theorem 4.2 (*Bounds of IFE Shape Functions*)**.** *There exists a constant C, independent of interface location, such that*

$$|\phi_{i,T}|_{k,\infty,T} \leqslant Ch^{-k}, \quad i \in \mathcal{I}, \quad k = 0, 1, 2, \quad \forall T \in \mathcal{T}_h^i. \tag{4.18}$$

Lemma 4.3 (*Partition of Unity*)**.** *For every interface element $T \in \mathcal{T}_h^i$, we have*

$$\sum_{i\in\mathcal{I}} \phi_{i,T}(X) = 1, \quad \forall X \in T. \tag{4.19}$$

Now, on every interface element T, for each $i \in \mathcal{I}$, we choose arbitrary points $\overline{X}_i \in l$ to construct two vector functions:

$$\begin{aligned} \boldsymbol{\Lambda}_s(X) = \sum_{i\in\mathcal{I}} (M_i - X)\phi_{i,T}^s(X) + \sum_{i\in\mathcal{I}^{s'}} (\overline{M}^s(F) - I)^T(M_i - \overline{X}_i)\phi_{i,T}^s(X) \\ + \frac{1}{h}\sum_{i\in\mathcal{I}^{int}} \int_{b_i\cap T^{s'}} (\overline{M}^s(F) - I)^T(P - \overline{X}_i)\phi_{i,T}^s(X)ds(P), \quad \text{if } X \in T_p^s, \end{aligned} \tag{4.20}$$

where $s = \pm$ and $p = curve$ or $line$. By Lemma 3.4 in [16], $\boldsymbol{\Lambda}_s(X)$ is well defined since it is independent of location of $\overline{X}_i \in l, i \in \mathcal{I}$. We can simplify $\boldsymbol{\Lambda}_s(X)$ further by the partition of unity:

$$\begin{aligned} \boldsymbol{\Lambda}_s(X) = \sum_{i\in\mathcal{I}} M_i\phi_{i,T}^s(X) - X + \sum_{i\in\mathcal{I}^{s'}} (\overline{M}^s(F) - I)^T(M_i - \overline{X}_i)\phi_{i,T}^s(X), \\ + \frac{1}{h}\sum_{i\in\mathcal{I}^{int}} \int_{b_i\cap T^{s'}} (\overline{M}^s(F) - I)^T(P - \overline{X}_i)\phi_{i,T}^s(X)ds(P), \end{aligned} \tag{4.21}$$

from which we have $\mathbf{\Lambda}_s(X) \in [\Pi_T]^2$, since $\phi^s_{i,T}(X) \in \Pi_T$, $s = \pm$, for $i \in \mathcal{I}$. Moreover, by the independence of $\overline{X}_i$, $i \in \mathcal{I}$, we could interchange $\overline{X}_i$ with an arbitrary fixed point $\overline{X} \in l$ and obtain

$$\begin{aligned}\mathbf{\Lambda}_s(X) =& \sum_{i\in\mathcal{I}^s\cup\mathcal{I}^{int}} (M_i - \overline{X})\phi^s_{i,T} + \sum_{i\in\mathcal{I}^{s'}} (\overline{M}^s(F))^T(M_i - \overline{X})\phi^s_{i,T} - X + \overline{X}\sum_{i\in\mathcal{I}}\phi^s_{i,T} \\ &+ (\overline{M}^s(F) - I)^T \sum_{i\in\mathcal{I}^{int}} \left(\frac{1}{h}\int_{b_i\cap T^{s'}} (P - \overline{X})ds(P)\right)\phi^s_{i,T}(X).\end{aligned} \tag{4.22}$$

By the identity $\frac{1}{h}\int_{b_i\cap T^+}(P-\overline{X})ds(P) + \frac{1}{h}\int_{b_i\cap T^-}(P-\overline{X})ds(P) = (M_i - \overline{X})$, $i \in \mathcal{I}^{int}$, (4.22) yields

$$\begin{aligned}\mathbf{\Lambda}_s(X) =& \sum_{i\in\mathcal{I}^s}(M_i - \overline{X})\phi^s_{i,T} + \sum_{i\in\mathcal{I}^{s'}\cup\mathcal{I}^{int}} (\overline{M}^s(F))^T(M_i - \overline{X})\phi^s_{i,T} - \mathbf{p}_0(X) \\ &- (\overline{M}^s(F) - I)^T \sum_{i\in\mathcal{I}^{int}} \left(\frac{1}{h}\int_{b_i\cap T^{s}} (P - \overline{X})ds(P)\right)\phi^s_{i,T}(X),\end{aligned} \tag{4.23}$$

where $\mathbf{p}_0(X) = X - \overline{X}\sum_{i\in\mathcal{I}}\phi^s_{i,T} = X - \overline{X}$, $s = \pm$, by the partition of unity. We consider a vector function

$$\boldsymbol{\psi}_0(X) = \begin{cases} \boldsymbol{\psi}_0^+(X) = \mathbf{p}_0(X), & \text{if } X \in T^+_p, \\ \boldsymbol{\psi}_0^-(X) = (\overline{M}^+(F))^T\mathbf{p}_0(X), & \text{if } X \in T^-_p, \end{cases} \tag{4.24}$$

where $p = curve$ or $line$ and $\overline{X}$ is an arbitrary point fixed on l.

Lemma 4.4. *For any point $\overline{X} \in l$, the vector function $\boldsymbol{\psi}_0$ defined by (4.24) belongs to $\left[S^{int}_h(T)\right]^2$.*

Proof. It suffices to verify that $\boldsymbol{\psi}_0$ satisfies the conditions (4.3) and (4.4). First it is easy to see $\partial_{xx}(\boldsymbol{\psi}^+_0) = \partial_{xx}(\boldsymbol{\psi}^-_0) = \mathbf{0}$, $s = \pm$. Besides, for any $\overline{X}' \in l$, Lemma 3.3 in [16] implies that $\boldsymbol{\psi}^-_0(\overline{X}') - \boldsymbol{\psi}^+_0(\overline{X}') = \left(\overline{M}^+(F) - I\right)^T\left(\overline{X}' - \overline{X}\right) = 0$, and hence $\boldsymbol{\psi}_0$ satisfies (4.3). Finally, Lemma 3.3 in [16] also shows that

$$\beta^-\nabla\boldsymbol{\psi}^-_0(F)\cdot\mathbf{v}(F) = \beta^-\left(\overline{M}^+(F)\right)^T\mathbf{v}(F) = \beta^+\mathbf{v}(F) = \beta^+\nabla\boldsymbol{\psi}^+_0(F)\cdot\mathbf{v}(F).$$

Therefore $\boldsymbol{\psi}_0$ satisfies (4.4). □

Now we consider an auxiliary piecewise vector function given by

$$\mathbf{\Lambda}(X) = \begin{cases} \mathbf{\Lambda}^+(X) = \mathbf{\Lambda}_+(X) & \text{if } X \in T^+_p, \\ \mathbf{\Lambda}^-(X) = (\overline{M}^+(F))^T\mathbf{\Lambda}_-(X) & \text{if } X \in T^-_p, \end{cases} \tag{4.25}$$

where $p = curve$ or $line$.

Theorem 4.3. *$\mathbf{\Lambda}(X)$ defined by (4.25) is in $\left[S^{int}_h(T)\right]^2$ and*

$$\int_{b_i}\mathbf{\Lambda}(X)ds(X) = \mathbf{0}, \ \forall i \in \mathcal{I}. \tag{4.26}$$

Proof. First, by comparing the coefficients of $\phi^s_{i,T}$ in $\mathbf{\Lambda}_s$ in (4.22) for $s = +$ and $\phi^s_{i,T}$ in $\mathbf{\Lambda}_s$ in (4.23) for $s = -$ and using Lemma 4.4, we have

$$\begin{aligned}\mathbf{\Lambda} =& \sum_{j\in\mathcal{I}^+\cup\mathcal{I}^{int}}(M_i - \overline{X})\phi_{j,T} + \sum_{j\in\mathcal{I}^-}(\overline{M}^+(F))^T(M_j - \overline{X})\phi_{j,T} - \boldsymbol{\psi}_0 \\ &+ (\overline{M}^+(F) - I)^T\sum_{j\in\mathcal{I}^{int}}\left(\frac{1}{h}\int_{b_j\cap T^-}(P - \overline{X})ds(P)\right)\phi_{j,T}\end{aligned} \tag{4.27}$$

which is actually a linear combination of $(\phi_{j,T}, 0)^T$, $(0, \phi_{j,T})^T$, and $\boldsymbol{\psi}_0$. Therefore $\mathbf{\Lambda} \in \left[S^{int}_h(T)\right]^2$. Next for $i \in \mathcal{I}^s$, $s = \pm$, it is easy to show (4.26). And for $i \in \mathcal{I}^{int}$, by (4.27), we have

$$\begin{aligned}\int_{b_i}\mathbf{\Lambda}(X)ds(X) =&(M_i - \overline{X}) - \frac{1}{h}\int_{b_i\cap T^+}(X - \overline{X})ds(X) - (\overline{M}^+(F))^T\frac{1}{h}\int_{b_i\cap T^-}(X - \overline{X})ds(X) \\ &+ (\overline{M}^+(F) - I)^T\left(\frac{1}{h}\int_{b_i\cap T^-}(P - \overline{X})ds(P)\right) = \mathbf{0}. \quad \square\end{aligned}$$

Theorem 4.4. *On every interface element $T \in \mathcal{T}_h^i$ we have*

$$\sum_{i\in\mathcal{I}}(M_i - X)\phi^s_{i,T}(X) + \sum_{i\in\mathcal{I}^{s'}}(\overline{M}^s(F) - I)^T(M_i - \overline{X}_i)\phi^s_{i,T}(X) + \frac{1}{h}\sum_{i\in\mathcal{I}^{int}}\int_{b_i\cap T^{s'}}(\overline{M}^s(F) - I)^T(P - \overline{X}_i)\phi^s_{i,T}(X)ds(P) = \mathbf{0}, \quad \forall X \in T^s_p, \tag{4.28}$$

and

$$\sum_{i\in\mathcal{I}}(M_i - X)\partial_d\phi^s_{i,T}(X) + \sum_{i\in\mathcal{I}^{s'}}\left[(\overline{M}^-(F) - I)^T(M_i - \overline{X}_i)\partial_d\phi^s_{i,T}(X)\right] + \sum_{i\in\mathcal{I}^{int}}\left(\frac{1}{h}\int_{b_i\cap T^s}(\overline{M}^s(F) - I)^T(P - \overline{X}_i)ds(P)\right)\partial_d\phi^s_{i,T}(X) - \mathbf{e}_d = \mathbf{0}, \ \forall X \in T^s_p, \tag{4.29}$$

where $s = \pm$, $p = curve$ or $line$ and $d = 1, 2$, $\partial_1 = \partial_x$, $\partial_2 = \partial_y$ are partial differential operators, and $\mathbf{e}_d$, $d = 1, 2$ is the canonical dth unit vector in $\mathbb{R}^2$.

Proof. The identity (4.28) follows from Theorem 4.3 and the unisolvence, and (4.29) is the derivative of (4.28). □

5. Optimal approximation capabilities of IFE spaces

In this section, we show the optimal approximation capabilities for two classes of IFE spaces defined by curved interface and its line approximation, respectively. This is achieved by deriving error bounds for the interpolation in IFE spaces.

We start from the local interpolation operator $I_{h,T} : C^0(T) \to S_h(T)$ on an element $T \in \mathcal{T}_h$:

$$I_{h,T}u(X) = \begin{cases} \sum_{i\in\mathcal{I}}\left(\frac{1}{|b_i|}\int_{b_i} uds\right)\psi_{i,T}(X), & \text{if } T \in \mathcal{T}_h^n, \\ \sum_{i\in\mathcal{I}}\left(\frac{1}{|b_i|}\int_{b_i} uds\right)\phi_{i,T}(X), & \text{if } T \in \mathcal{T}_h^i. \end{cases} \tag{5.1}$$

Then, as usual, the global IFE interpolation $I_h : C^0(\Omega) \to S_h(\Omega)$ can be defined piecewisely:

$$(I_h u)|_T = I_{h,T}u, \quad \forall T \in \mathcal{T}_h. \tag{5.2}$$

First for the local interpolation $I_{h,T}u$ on every non-interface element $T \in \mathcal{T}_h^n$, the standard argument [21] yields

$$\|I_{h,T}u - u\|_{0,T} + h|I_{h,T}u - u|_{1,T} \leqslant Ch^2|u|_{2,T}, \ \forall u \in H^2(T). \tag{5.3}$$

On each interface element $T \in \mathcal{T}_h^i$, for $s = \pm$, $i \in \mathcal{I}$, we consider two functions $E_i : b_i \times T_{non} \to \mathbb{R}$ and $F_i : b_i \times T_{non} \to \mathbb{R}$ such that

$$E_i(P, X) = \begin{cases} ((M^s(\widetilde{Y}_i) - \overline{M}^s(F))\nabla u^s(X)) \cdot (P - \overline{X}_i), & \text{if } P \in b_i \cap T^{s'}, X \in T^s_{non}, \\ 0, & \text{otherwise}, \end{cases}$$
$$F_i(P, X) = \begin{cases} \left((\overline{M}^s(F) - I)\nabla u^s(X)\right) \cdot (\widetilde{Y}_i - \overline{X}_i), & \text{if } P \in b_i \cap T^{s'}, X \in T^s_{non}, \\ 0, & \text{otherwise}, \end{cases} \tag{5.4}$$

where $\widetilde{Y}_i = \widetilde{Y}_i(P, X)$ and $\overline{X}_i \in l$, $i \in \mathcal{I}$. We note that E_i and F_i are piecewisely defined on $b_i \times T_{non}$. Furthermore, integrating for $i \in \mathcal{I}^{s'} \cup \mathcal{I}^{int}$, (5.4) leads to the following two functions $\mathcal{E}_i : T_{non} \to \mathbb{R}$ and $\mathcal{F}_i : T_{non} \to \mathbb{R}$:

$$\mathcal{E}_i(X) = \frac{1}{h}\int_{b_i\cap T^{s'}} E_i(P, X)ds(P), \quad \mathcal{F}_i(X) = \frac{1}{h}\int_{b_i\cap T^{s'}} F_i(P, X)ds(P), \quad \text{if } X \in T^s_{non}. \tag{5.5}$$

Note that $\mathcal{E}_i$ and $\mathcal{F}_i$ are also piecewisely defined on T. Their estimates are given in the following theorem.

Lemma 5.1. *There exists a constant $C > 0$ independent of the interface location such that the following estimates hold for every $T \in \mathcal{T}_h^i$ and $u \in PC^2_{int}(T)$:*

$$\|\mathcal{E}_i\|_{0,T^s_{non}} \leqslant Ch^2|u|_{1,T^s}, \quad \|\mathcal{F}_i\|_{0,T^s_{non}} \leqslant Ch^2|u|_{1,T^s}, \quad s = \pm. \tag{5.6}$$

Proof. By the Lemma 5.7 in [16], for fixed $P \in b_i \cap T^{s'}$, we have

$$\|E_i(P,\cdot)\|_{0,T^s_{non}} \leqslant Ch^2|u|_{1,T^s}, \quad \|F_i(P,\cdot)\|_{0,T^s_{non}} \leqslant Ch^2|u|_{1,T^s}. \tag{5.7}$$

Then, the estimate (5.6) follows from the same arguments as in the proof for Lemma 3.1. □

We now derive expansions for the interpolation error. The first group of expansions are for the interpolation error at $X \in T_{non}$ given in the following theorem.

Theorem 5.1. *Let $T \in \mathcal{T}^i_h$ and $u \in PC^2_{int}(T)$. Then for any $\overline{X}_i \in l$, $i \in \mathcal{I}$, we have*

$$I_{h,T}u(X) - u(X) = \sum_{i\in\mathcal{I}^{s'}\cup\mathcal{I}^{int}} (\mathcal{E}_i + \mathcal{F}_i)\phi_{i,T}(X) + \sum_{i\in\mathcal{I}} \mathcal{R}_i\phi_{i,T}(X), \ \forall X \in T^s_{non} \cap T^s_p, \ s = \pm, \tag{5.8a}$$

$$\partial_d(I_{h,T}u(X) - u(X)) = \sum_{i\in\mathcal{I}^{s'}\cup\mathcal{I}^{int}} (\mathcal{E}_i + \mathcal{F}_i)\partial_d\phi_{i,T}(X) + \sum_{i\in\mathcal{I}} \mathcal{R}_i\partial_d\phi_{i,T}(X), \ \forall X \in T^s_{non} \cap T^s_p, \ s = \pm, \tag{5.8b}$$

where $p = curve$ or $line$, $d = 1$ or 2, $\mathcal{R}^s_i$ and $\mathcal{E}_i$, $\mathcal{F}_i$ are given by (3.9), and (5.5), respectively.

Proof. First, for $X \in T^s_{non} \cap T^s_p$, $s = \pm$, substituting the expansion (3.6), (3.7) and (3.8) into the IFE interpolation (5.1) and using the partition of unity yields

$$\begin{aligned} I_{h,T}u(X) =& u^s(X) + \nabla u^s(X)\cdot\sum_{i\in\mathcal{I}}(M_i - X)\phi^s_{i,T}(X) + \sum_{i\in\mathcal{I}} R^s_i\phi^s_{i,T}(X) \\ &+ \sum_{i\in\mathcal{I}^{s'}} \frac{1}{h}\int_{b_i} \left(\left(M^s(\widetilde{Y}_i) - I\right)\nabla u^s(X)\right)\cdot(P - \widetilde{Y}_i)ds(P)\phi^s_{i,T}(X) \\ &+ \sum_{i\in\mathcal{I}^{int}} \frac{1}{h}\int_{b_i\cap T^{s'}} \left(\left(M^s(\widetilde{Y}_i) - I\right)\nabla u^s(X)\right)\cdot(P - \widetilde{Y}_i)ds(P)\phi^s_{i,T}(X), \ s = \pm. \end{aligned} \tag{5.9}$$

Applying (4.28) in Theorem 4.4, we have

$$\begin{aligned} I_{h,T}u(X) =& u^s(X) - \sum_{i\in\mathcal{I}^{s'}} \frac{1}{h}\int_{b_i} \left(\left(\overline{M}^s(F) - I\right)\nabla u^s(X)\right)\cdot(P - \overline{X}_i)ds(P)\phi_{i,T}(X) + \sum_{i\in\mathcal{I}} R^s_i\phi_{i,T}(X) \\ &- \sum_{i\in\mathcal{I}^{int}} \frac{1}{h}\int_{b_i\cap T^{s'}} \left(\left(\overline{M}^s(F) - I\right)\nabla u^s(X)\right)\cdot(P - \overline{X}_i)ds(P)\phi^s_{i,T}(X) \\ &+ \sum_{i\in\mathcal{I}^{s'}} \frac{1}{h}\int_{b_i} \left(\left(M^s(\widetilde{Y}_i) - I\right)\nabla u^s(X)\right)\cdot(P - \widetilde{Y}_i)ds(P)\phi_{i,T}(X) \\ &+ \sum_{i\in\mathcal{I}^{int}} \frac{1}{h}\int_{b_i\cap T^{s'}} \left(\left(M^s(\widetilde{Y}_i) - I\right)\nabla u^s(X)\right)\cdot(P - \widetilde{Y}_i)ds(P)\phi_{i,T}(X), \ s = \pm. \end{aligned} \tag{5.10}$$

Then substituting $P - \overline{X}_i = (P - \widetilde{Y}_i) + (\widetilde{Y}_i - \overline{X}_i)$ into (5.10) yields (5.8a). Furthermore, applying the expansions (3.6), (3.7) in $\partial_d I_{h,T}u(X) = \sum_{i\in\mathcal{I}}\frac{1}{h}\int_{b_i} u(P)ds(P)\partial_d\phi_{i,T}(X)$, $d = 1, 2$, yields

$$\begin{aligned} \partial_d I_{h,T}u(X) =& \nabla u^s(X)\cdot\sum_{i\in\mathcal{I}}(M_i - X)\partial_d\phi^s_{i,T}(X) + \sum_{i\in\mathcal{I}} R^s_i\partial_d\phi^s_{i,T}(X) \\ &+ \sum_{i\in\mathcal{I}^{s'}} \frac{1}{h}\int_{b_i} \left(\left(M^s(\widetilde{Y}_i) - I\right)\nabla u^s(X)\right)\cdot(P - \widetilde{Y}_i)ds(P)\partial_d\phi^s_{i,T}(X) \\ &+ \sum_{i\in\mathcal{I}^{int}} \frac{1}{h}\int_{b_i\cap T^{s'}} \left(\left(M^s(\widetilde{Y}_i) - I\right)\nabla u^s(X)\right)\cdot(P - \widetilde{Y}_i)ds(P)\partial_d\phi^s_{i,T}(X), \ s = \pm. \end{aligned} \tag{5.11}$$

Finally, using (4.29) and similar argument above, we have (5.8b). □

The second group of expansions are for $X \in T_{int}$ which is much simpler. Using (3.13) in $I_{h,T}u(X)$ defined in (5.1) and the partition of unity, we have

$$I_{h,T}u(X) - u(X) = \sum_{i\in\mathcal{I}} \mathcal{R}_i\phi_{i,T}(X), \qquad \forall X \in T_{int}, \tag{5.12a}$$

$$\partial_d I_{h,T}u(X) - \partial_d u(X) = -\partial_d u(X) + \sum_{i\in\mathcal{I}} \mathcal{R}_i \partial_d \phi_{i,T}(X), \quad \forall X \in T_{int}, \ \ d = x, \ y. \tag{5.12b}$$

5.1. Curve partition

In this subsection, we derive error bounds for the interpolation in the IFE space defined according to the actual interface Γ on each interface element, i.e., the local IFE functions on each interface element T are defined by (4.2) with $T_p^s = T_{curve}^s$, $s = \pm$. We first derive an estimate for the IFE interpolation error on T_{non}.

Theorem 5.2. *There exists a constant $C > 0$ independent of the interface location such that for every $u \in PH^2_{int}(T)$ it holds*

$$\|I_{h,T}u - u\|_{0,T_{non}} + h|I_{h,T}u - u|_{1,T_{non}} \leqslant Ch^2(|u|_{1,T} + |u|_{2,T}), \ \ \forall T \in \mathcal{T}_h^i. \tag{5.13}$$

Proof. On each $T \in \mathcal{T}_h^i$, Theorems 4.2 and 5.1 show that there exists a constant C such that for every $u \in PC^2_{int}(T)$ we have

$$\|I_{h,T}u - u\|_{0,T^s_{non}} \leqslant C\left(\sum_{i\in\mathcal{I}^{s'}\cup\mathcal{I}^{int}} \left(\|\mathcal{E}_i\|_{0,T^s_{non}} + \|\mathcal{F}_i\|_{0,T^s_{non}}\right) + \sum_{i\in\mathcal{I}} \|\mathcal{R}_i\|_{0,T^s_{non}}\right), \tag{5.14}$$

$$\|\partial_d(I_{h,T}u - u)\|_{0,T^s_{non}} \leqslant \frac{C}{h}\left(\sum_{i\in\mathcal{I}^{s'}\cup\mathcal{I}^{int}} \left(\|\mathcal{E}_i\|_{0,T^s_{non}} + \|\mathcal{F}_i\|_{0,T^s_{non}}\right) + \sum_{i\in\mathcal{I}} \|\mathcal{R}_i\|_{0,T^s_{non}}\right), \ d = 1, 2. \tag{5.15}$$

Then, applying Lemmas 5.1 and 3.1 to the two estimates above yields

$$\|I_{h,T}u - u\|_{0,T^s_{non}} + h|I_{h,T}u - u|_{1,T^s_{non}} \leqslant Ch^2(|u|_{1,T} + |u|_{2,T}), \ s = \pm.$$

The estimate (5.13) for $u \in PC^2_{int}(T)$ follows from summing the inequality above for $s = -, +$. And the estimate (5.13) for $u \in PH^2_{int}(T)$ follows from the density hypothesis **(H4)**. □

Furthermore, for the estimation on T_{int}, using the fact $u \in PW^{1,6}_{int}(T)$, we have

Theorem 5.3. *There exists a constant $C > 0$ independent of the interface location such that for every $u \in PH^2_{int}(T)$ it holds*

$$\|I_{h,T}u - u\|_{0,T_{int}} + h|I_{h,T}u - u|_{1,T_{int}} \leqslant Ch^2\|u\|_{1,6,T}, \ \ \forall T \in \mathcal{T}_h^i. \tag{5.16}$$

Proof. Firstly, Theorem 4.2 and (3.15) imply that

$$\|\mathcal{R}_i\,\phi_{i,T}\|_{0,T_{int}} \leqslant Ch^2\|u\|_{1,6,T} \quad \text{and} \quad \|\mathcal{R}_i\,\partial_d\phi_{i,T}\|_{0,T_{int}} \leqslant Ch\|u\|_{1,6,T}.$$

where $d = x, y$. Using the Hölder's inequality again, we have

$$\left(\int_{T_{int}} (\partial_d u)^2 dX\right)^{1/2} \leqslant \left(\int_{T_{int}} 1^{3/2} dX\right)^{1/3} \left(\int_{T_{int}} (\partial_d u)^6 dX\right)^{1/6} \leqslant Ch\|u\|_{1,6,T}.$$

Then, (5.16) follows from applying estimates above together with the density hypothesis **(H4)** to expansions in (5.8). □

Finally we can prove the following global estimate for the IFE interpolation by summing the local estimate over all the elements.

Theorem 5.4. *For any $u \in PH^2_{int}(\Omega)$, the following estimate of interpolation error holds*

$$\|I_h u - u\|_{0,\Omega} + h|I_h u - u|_{1,\Omega} \leqslant Ch^2\|u\|_{2,\Omega}. \tag{5.17}$$

Proof. Putting (5.13) and (5.16) together, we have

$$\|I_{h,T}u - u\|_{0,T} + h|I_{h,T}u - u|_{1,T} \leqslant Ch^2(\|u\|_{2,T} + \|u\|_{1,6,T}), \ \ \forall T \in \mathcal{T}_h^i. \tag{5.18}$$

Then, by summing (5.18) and (5.3) over all the interface and non-interface elements, we have

$$\|I_h u - u\|_{0,\Omega} + h|I_h u - u|_{1,\Omega} \leqslant Ch^2(\|u\|_{2,\Omega} + \|u\|_{1,6,\Omega}).$$

We note the following estimate from [23] that for any $p \geqslant 2$

$$\|u\|^2_{1,p,\Omega^s} \leqslant Cp\,\|u\|^2_{2,\Omega^s}, \ \ s = \pm.$$

Combining the two inequalities above leads to (5.17). □

5.2. Line partition

In this subsection, we derive error bounds for the interpolation in the IFE space constructed by using the straight line to approximate the actual interface Γ on each interface element, i.e., the local IFE functions on each interface element T are defined by (4.2) with $T_p^s = T_{line}^s$, $s = \pm$. Let $\overline{T}^s = T_{non}^s \cap T_{line}^s$ and $\widetilde{T}$ be the subset of T sandwiched between Γ and l. Because $\overline{T}^s \subseteq T_{non}$, $s = \pm$, by the same arguments for Theorem 5.2, we have

$$\|I_{h,T}u - u\|_{0,\overline{T}^s} + h|I_{h,T}u - u|_{1,\overline{T}^s} \leqslant Ch^2(|u|_{1,T} + |u|_{2,T}), \quad s = \pm, \ \forall\, T \in \mathcal{T}_h^i. \tag{5.19}$$

Similarly, the estimate (5.16) is also valid for the IFE space constructed using the straight line to approximate the actual interface Γ.

For $\widetilde{T}$, we note that there exists a constant C such that $|\widetilde{T}| \leqslant Ch^3$. Then, applying the same arguments as those for Theorem 5.3, we can prove the following theorem.

Theorem 5.5. *There exists a constant $C > 0$ independent of the interface location such that for every $u \in PH_{int}^2(T)$ it holds*

$$\|I_{h,T}u - u\|_{0,\widetilde{T}} + h|I_{h,T}u - u|_{1,\widetilde{T}} \leqslant Ch^2\|u\|_{1,6,T}, \quad s = \pm, \ \forall\, T \in \mathcal{T}_h^i. \tag{5.20}$$

For each interface element $T \in \mathcal{T}_h^i$, because

$$T = \left(\overline{T}^- \cup \overline{T}^+ \cup \widetilde{T} \cup T_{int}\right),$$

we can put estimates above together to have

$$\|I_{h,T}u - u\|_{0,T} + h|I_{h,T}u - u|_{1,T} \leqslant Ch^2(\|u\|_{2,T} + \|u\|_{1,6,T}), \quad \forall\, T \in \mathcal{T}_h^i. \tag{5.21}$$

Finally, by the same arguments for Theorem 5.4, we can derive the global interpolation error estimate given in the following theorem for the IFE space constructed by using the straight line to approximate the actual interface Γ.

Theorem 5.6. *For any $u \in PH_{int}^2(\Omega)$, the following estimation of interpolation error holds*

$$\|I_{h,T}u - u\|_{0,\Omega} + h|I_{h,T}u - u|_{1,\Omega} \leqslant Ch^2\|u\|_{2,\Omega}. \tag{5.22}$$

Remark 5.1. The estimate (5.22) is also derived in Theorem 3.12 of [14] through an argument based on the interpolation error bounds for the rotated-Q_1 IFE space with the Lagrange type degrees of freedom.

6. Numerical examples

In this section we present some numerical results to demonstrate features of the interpolation and Galerkin solution for IFE spaces discussed in the previous sections. We shall consider two examples with different interface shapes. The first example is the same as the one in [24]. Specifically, the solution domain is $\Omega = (-1, 1) \times (-1, 1)$ which is divided into two subdomains Ω^- and Ω^+ by a circular interface Γ with radius $r_0 = \pi/6.28$ such that $\Omega^- = \{(x, y) : x^2 + y^2 < r_0^2\}$. Functions f and g in (1.1) are given such that the exact solution to interface problem described by (1.1)–(1.4) is given by the following formula:

$$u(x, y) = \begin{cases} \dfrac{1}{\beta^-} r^\alpha, & (x, y) \in \Omega^-, \\ \dfrac{1}{\beta^+} r^\alpha + \left(\dfrac{1}{\beta^-} - \dfrac{1}{\beta^+}\right) r_0^\alpha, & (x, y) \in \Omega^+, \end{cases} \tag{6.1}$$

where $r = \sqrt{x^2 + y^2}$ and $\alpha = 5$. The second example has a flower-like interface, which is also tested on the same domain $\Omega = (-1, 1) \times (-1, 1)$, as illustrated in Fig. 6.1. The exact solution is given by

$$u(x, y) = \begin{cases} \dfrac{(x^2 + y^2)^2(1 + 0.4\sin(6\tan^{-1}(y/x))) - 0.3}{\beta^-}, & (x, y) \in \Omega^-, \\ \dfrac{(x^2 + y^2)^2(1 + 0.4\sin(6\tan^{-1}(y/x))) - 0.3}{\beta^+}, & (x, y) \in \Omega^+. \end{cases} \tag{6.2}$$

Although numerical examples for two different interface shapes are presented here, our extensive numerical experiments and error analysis indicate that the proposed IFE spaces can be constructed and they can perform optimally for general interfaces as long as the hypothesis **(H1)–(H4)** are satisfied. In our numerical examples reported here, we construct IFE spaces by rotated-Q_1 polynomials defined with the actual interface curve, and the flux continuity (4.4) is enforced at the midpoint F of the curve $\Gamma \cap T$ for constructing IFE shape functions. To avoid redundancy, we only present numerical result

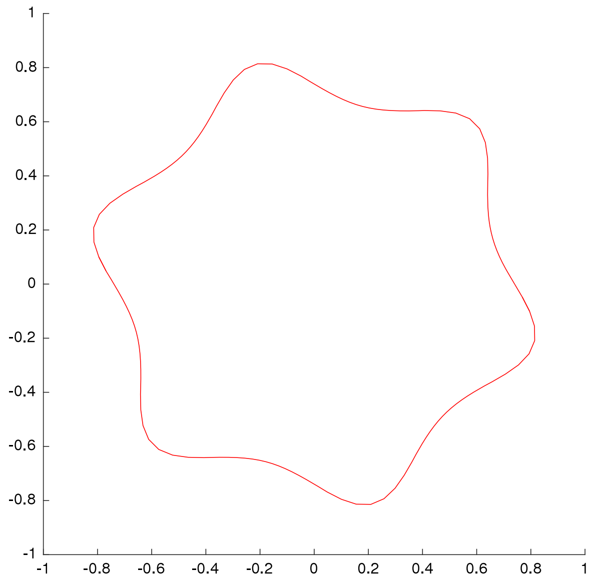

Fig. 6.1. The flower-like interface with 6 petals.

Table 1
Interpolation errors and rates for the rotated-Q_1 IFE function, $\beta^- = 1$ and $\beta^+ = 10\,000$ for the circular interface.

h	$\|u - I_h u\|_{0,\Omega}$	Rate	$\|u - I_h u\|_{1,\Omega}$	Rate
1/20	6.3804E−4		2.7693E−2	
1/40	1.6776E−4	1.9272	1.4436E−2	0.9399
1/80	4.3557E−5	1.9454	7.4385E−3	0.9566
1/160	1.1100E−5	1.9723	3.7803E−3	0.9765
1/320	2.8083E−6	1.9828	1.9060E−3	0.9880
1/640	7.0568E−7	1.9926	9.5704E−4	0.9939
1/1280	1.7692E−7	1.9959	4.7959E−4	0.9968

Table 2
Galerkin solution errors and rates for the rotated-Q_1 IFE solution, $\beta^- = 1$, $\beta^+ = 10\,000$ for the circular interface.

h	$\|u - u_h\|_{0,\Omega}$	Rate	$\|u - u_h\|_{1,\Omega}$	Rate
1/20	1.4221E−3		2.8852E−2	
1/40	3.4863E−4	2.0283	1.4822E−2	0.9610
1/80	8.5873E−5	2.0214	7.5721E−3	0.9689
1/160	2.1046E−5	2.0286	3.8057E−3	0.9925
1/320	5.7133E−6	1.8812	1.9154E−3	0.9905
1/640	1.4044E−6	2.0243	9.5891E−4	0.9982
1/1280	3.4603E−7	2.0210	4.8004E−4	0.9982

of relatively large coefficient jump, i.e, $\beta^- = 1$, $\beta^+ = 10\,000$. Similar behavior are observed for the reverse of jump values $\beta^- = 10\,000$ and $\beta^+ = 1$ and for small coefficient jumps.

Since IFE functions on each interface element $T \in \mathcal{T}_h^i$ are defined as piecewise rotated-Q_1 polynomials by two subelements sharing a curved boundary $\Gamma \cap T$, integrations over these curve subelements require special attentions when assembling the local matrix and vector. These two subelements can be such that one is a curved triangle and the other one is a curved pentagon, or they are two curved quadrilaterals, all of them just have one curved edge. For the quadratures on the curved pentagon, we can partition it further into a straight edge triangle and a curved edge quadrilateral. Then we use the standard isoparametric mapping for integrations on curved triangles and quadrilaterals.

Tables 1, 3 and 2, 4 present interpolation errors $u - I_h u$ and Galerkin IFE solution errors $u - u_h$ for both examples, respectively. The errors are measured in terms of the L^2 and the semi-H^1 norms generated over a sequence of meshes with size h from 1/20 to 1/1280. The rates listed in these tables are estimated by the numerical results generated on two consecutive meshes.

Data in Tables 1 and 3 clearly shows the optimal convergence rate for the IFE interpolation for both examples, which agrees with our theoretical analysis before. The IFE solutions u_h in Tables 2 and 4 are generated by the standard Galerkin

Table 3
Interpolation errors and rates for the rotated-Q_1 IFE function, $\beta^- = 1$ and $\beta^+ = 10\,000$ for the flower interface.

h	$\|u - I_h u\|_{0,\Omega}$	Rate	$|u - I_h u|_{1,\Omega}$	Rate
1/20	4.3903-3		2.0254E−1	
1/40	1.1592E−3	1.9212	1.0185E−1	0.9917
1/80	2.9131E−4	1.9925	5.0519E−2	1.0116
1/160	7.3475E−5	1.9872	2.5369E−2	0.9938
1/320	1.8425E−5	1.9956	1.2687E−2	0.9998
1/640	4.6166E−6	1.9968	6.3506E−3	0.9983
1/1280	1.1551E−6	1.9988	3.1759E−3	0.9997

Table 4
Galerkin solution errors and rates for the rotated-Q_1 IFE solution, $\beta^- = 1$, $\beta^+ = 10\,000$ for the flower interface.

h	$\|u - u_h\|_{0,\Omega}$	Rate	$|u - u_h|_{1,\Omega}$	Rate
1/20	7.6399E−3		2.2195E−1	
1/40	2.1394E−3	1.8363	1.0926E−1	1.0225
1/80	4.9755E−4	2.1043	5.3539E−2	1.0291
1/160	1.2497E−4	1.9933	2.6142E−2	1.0342
1/320	3.1951E−5	1.9676	1.3027E−2	1.0048
1/640	7.2910E−6	2.1317	6.4176E−3	1.0251
1/1280	1.8670E−6	1.9654	3.1966E−3	1.0055

formulation with a discrete bilinear form [5,6,14] without any penalties on interface edges such as those used in the partially penalized IFE methods in [24]. This means the IFE method used to generate data in Tables 2 and 4 is simpler than the one discussed in [24]. The data in Tables 2 and 4 demonstrates that the classic scheme using the nonconforming IFE spaces developed in this article performs optimally also for both examples. Finally, we refer readers to [13,14] for numerical results generated with the nonconforming IFE spaces defined with the line approximation.

References

[1] Z. Li, The immersed interface method using a finite element formulation, Appl. Numer. Math. 27 (3) (1998) 253–267.
[2] Y. Gong, B. Li, Z. Li, Immersed-interface finite-element methods for elliptic interface problems with nonhomogeneous jump conditions, SIAM J. Numer. Anal. 46 (1) (2007/08) 472–495.
[3] X. He, T. Lin, Y. Lin, Immersed finite element methods for elliptic interface problems with non-homogeneous jump conditions, Int. J. Numer. Anal. Model. 8 (2) (2011) 284–301.
[4] S. Hou, X.-D. Liu, A numerical method for solving variable coefficient elliptic equation with interfaces, J. Comput. Phys. 202 (2) (2005) 411–445.
[5] Z. Li, T. Lin, Y. Lin, R.C. Rogers, An immersed finite element space and its approximation capability, Numer. Methods Partial Differential Equations 20 (3) (2004) 338–367.
[6] Z. Li, T. Lin, X. Wu, New Cartesian grid methods for interface problems using the finite element formulation, Numer. Math. 96 (1) (2003) 61–98.
[7] X. He, Bilinear Immersed Finite Elements for Interface Problems (Ph.D. thesis), Virginia Polytechnic Institute and State University, 2009.
[8] X. He, T. Lin, Y. Lin, Approximation capability of a bilinear immersed finite element space, Numer. Methods Partial Differential Equations 24 (5) (2008) 1265–1300.
[9] T. Lin, Y. Lin, R. Rogers, M.L. Ryan, A rectangular immersed finite element space for interface problems, in: Scientific Computing and Applications, (Kananaskis, AB, 2000), in: Adv. Comput. Theory Pract., vol. 7, Nova Sci. Publ., Huntington, NY, 2001, pp. 107–114.
[10] T. Lin, X. Zhang, Linear and bilinear immersed finite elements for planar elasticity interface problems, J. Comput. Appl. Math. 236 (18) (2012) 4681–4699.
[11] D.Y. Kwak, K.T. Wee, K.S. Chang, An analysis of a broken P_1-nonconforming finite element method for interface problems, SIAM J. Numer. Anal. 48 (6) (2010) 2117–2134.
[12] T. Lin, D. Sheen, X. Zhang, A locking-free immersed finite element method for planar elasticity interface problems, J. Comput. Phys. 247 (2013) 228–247.
[13] T. Lin, D. Sheen, X. Zhang, Nonconforming immersed finite element methods for elliptic interface problems, 2015. arXiv:1510.00052.
[14] X. Zhang, Nonconforming Immersed Finite Element Methods for Interface Problems (Ph.D. Thesis), Virginia Polytechnic Institute and State University, 2013.
[15] J. Guzmán, N.A. Sánchez, M. Sarkis, A finite element method for high-contrast interface problems with error estimates independent of contrast, J. Sci. Comput. 73 (1) (2017) 330–365.
[16] R. Guo, T. Lin, A group of immersed finite element spaces for elliptic interface problems, IMA J. Numer. Anal. (2017). http://dx.doi.org/10.1093/imanum/drx074 (in press).
[17] S. Adjerid, R. Guo, T. Lin, High degree immersed finite element spaces by a least squares method, Int. J. Numer. Anal. Model. 14 (4–5) (2017) 604–626.
[18] H. Ji, J. Chen, Z. Li, A symmetric and consistent immersed finite element method for interface problems, J. Sci. Comput. 61 (3) (2014) 533–557.
[19] J. Xu, Estimate of the convergence rate of the finite element solutions to elliptic equation of second order with discontinuous coefficients, Natur. Sci. J. Xiangtan Univ. 1 (1982) 1–5.
[20] X. He, T. Lin, Y. Lin, A bilinear immersed finite volume element method for the diffusion equation with discontinuous coefficient, Commun. Comput. Phys. 6 (1) (2009) 185–202.
[21] R. Rannacher, S. Turek, Simple nonconforming quadrilateral Stokes element, Numer. Methods Partial Differential Equations 8 (2) (1992) 97–111.
[22] Z. Chen, J. Zou, Finite element methods and their convergence for elliptic and parabolic interface problems, Numer. Math. 79 (2) (1998) 175–202.
[23] X. Ren, J. Wei, On a two-dimensional elliptic problem with large exponent in nonlinearity, Trans. Amer. Math. Soc. 343 (2) (1994) 749–763.
[24] T. Lin, Y. Lin, X. Zhang, Partially penalized immersed finite element methods for elliptic interface problems, SIAM J. Numer. Anal. 53 (2) (2015) 1121–1144.